Ka-Band Site Characterization of the NASA Near Earth Network in Svalbard, Norway

R. Acosta[1], J. Morse[1], J. Nessel[1], M. Zemba[1], K. Tuttle[1],
A. Caroglanian[2], B. Younes[3] and Sten-Chirstian Pedersen[4]

[1]NASA Glenn Research Center
Cleveland, Ohio 44135
Phone: (216) 433-6640, Fax: (216) 433-6371, Email: racosta@grc.nasa.gov

[2]NASA Goddard Spaceflight Center
Greenbelt, Maryland 20771
*Phone: (*301) 286-4340*, Email:* armen.caroglanian-1@nasa.go

[3]NASA Headquarters
Washington, DC 20546-0001
*Phone: (*202) 358-2020*, Email: badri.younes-1@nasa.gov*

[4] Kongsberg Satellite Services AS, SvalSat
9171 Longyearbyen, Norway
Phone: +47 79 02 25 65, Email: stenp@ksat.no

Abstract

Critical to NASA's rapid migration toward Ka-Band is the comprehensive characterization of the communication channels at NASA's ground sites to determine the effects of the atmosphere on signal propagation and the network's ability to support various classes of users in different orbits. Accordingly, NASA has initiated a number of studies involving the ground sites of its Near Earth and Deep Space Networks. Recently, NASA concluded a memorandum of agreement (MOA) with the Norwegian Space Centre of the Kingdom of Norway and began a joint site characterization study to determine the atmospheric effects on Ka-Band links at the Svalbard Satellite Station in Norway, which remains a critical component of NASA's Near Earth Communication Network (NEN). System planning and design for Ka-band links at the Svalbard site cannot be optimally achieved unless measured attenuation statistics (e.g. cumulative distribution functions (CDF)) are obtained. In general, the CDF will determine the necessary system margin and overall system availability due to the atmospheric effects. To statistically characterize the attenuation statistics at the Svalbard site, NASA has constructed a ground-based monitoring station consisting of a multi-channel total power radiometer (25.5 – 26.5 GHz) and a weather monitoring station to continuously measure (at 1 second intervals) attenuation and excess noise (brightness temperature). These instruments have been tested in a laboratory environment as well as in an analogous outdoor climate (i.e. winter in Northeast Ohio), and the station was deployed in Svalbard, Norway in May 2011. The measurement campaign is planned to last a minimum of 3 years but not exceeding a maximum of 5 years.

I. Introduction

The purpose of the site characterization at the Svalbard site in Norway is to determine the expected Ka-Band performance of the Near Earth Network (NEN) ground stations with respect to atmospheric propagation effects. In particular, validation of the anticipated atmospheric-induced attenuation and increases in system temperature will be conducted by deploying a microwave radiometer specifically designed to measure the contribution of the atmosphere toward the Ka-Band link degradation. Conducting these measurements will directly provide: enhanced system planning through accurate determination of expected link availability at Ka-band, improved science mission planning by

managing expectations and maximizing mission success and data throughput, and necessary preparation for deployment of the NEN Ka-Band Polar Network.

Atmospheric effects on earth-space communication links are of great concern and become even more significant at Ka-Band frequencies as opposed to the more commonly used C-, X-, and Ku-Band. The reason for this concern is that, as frequency increases, the propagation path becomes more susceptible to losses in the troposphere (lower atmosphere). The principal effect on radio wave propagation in the troposphere is attenuation (absorption) of the signal caused by atmospheric gases (mainly water vapor and oxygen), hydrosols (suspended water droplets, e.g. haze, fog, and clouds), and precipitating water (rain) **[1]**. The total attenuation due to atmospheric gaseous absorption (AGA) is dominated by oxygen and water vapor, as the absorption lines of other trace gases are not significant for frequencies below 300 GHz.

A multifrequency radiometer is the optimal system to directly measure the absorption due to atmospheric gaseous and clouds at any given site when rain is not a dominant factor**[2, 3]**. Path attenuation, which includes clear air loss, is derived from the sky brightness temperature data collected by the radiometer. Radiometrically derived attenuation is a good estimate for low attenuation values (below 10 dB). In the absence of rain, a radiometer measures the attenuation due to clouds, water vapor and atmospheric gases, which, in a location such as Longyearbyen, Norway, is the dominant propagation-related attenuation phenomenon.

This paper is organized as follows: In section II, we describe the radiometer hardware and derive the formula for calculating the attenuation from the sky brightness temperature. Preliminary statistical results of attenuation and weather statistics are presented in section III. Section IV contains conclusive remarks and future work.

II. Ka-Band Radiometer Measured Performance

A multifrequency (25.5 – 26.5 GHz) microwave radiometer with a steerable horn antenna has been employed for the measurement of the sky brightness temperature in this study. **Figure 1** shows a picture of the radiometer hardware at the GRC laboratory (system check-out phase) and at it was deployed (operational site) at Longyearbyen, Norway. This ground-based radiometer is a single linearly polarized, super heterodyne, and Dicke-switched instrument. The central frequency of the radiometer is 26.0 GHz with an intermediate frequency bandwidth of 500 MHz. The half power beam width of the horn antenna is approximately 3^{o} at 26 GHz, and the sensitivity is 0.5 K for an integration time of 1 s. The voltage signal from the radiometer is fed into the low-pass filter/amplifier that determines the integration time of the radiometer. The signal from the low-pass filter is sent to a printer/recorder for viewing the data in real time and to a data collection board connected to the bus of the host computer that controls the data acquisition. The data collection board digitizes the radiometer output with 12 bit precision. The positions of the antenna in azimuth and elevation are recorded each time the radiometer signals are sampled. The detailed characteristics of the radiometer are summarized in **Table 1**.

The antenna noise temperature measured by the radiometer contains not only true sky brightness temperature but also the system noise temperature. The radiometer system noise temperature is very sensitive to thermal changes in the environment and so a Dicke reference load and a noise diode that serve as an internal calibration source for estimating the system noise temperature are used before a measurement is performed. In addition, the radiometer is absolutely calibrated by using the 'tipping curve' technique. This measurement under clear sky conditions is the most precise method of overall system calibration **[4].** The feed assembly and the antenna horn lens loss estimates shall be adjusted initially in this way, and likewise periodic checks of system calibration can be made.

Tipping Curve calibration is based on the assumption that, under clear sky conditions, the atmosphere is comprised of stratified layers of homogeneous distributions of water vapor and other gaseous elements. Thus the attenuation of a satellite signal will follow a secant law, therefore,

(1)

where $A(90^{o})$ is the zenith attenuation and θ is the elevation angle of the ground station.

By plotting A(θ) versus 1/sin(θ), a straight line is obtained which should have a zero intercept point. If the intersection differs from zero this indicates that a change in system calibration has occurred, and recalibration is required. Recalibration of the system is required when there is a change in the loss/reflection characteristics of the horn-input waveguide circuits, or a change in level of injected noise, which is more frequently the cause. A recalibration is performed by adjusting the calibration loss factor in the radiometer equations.

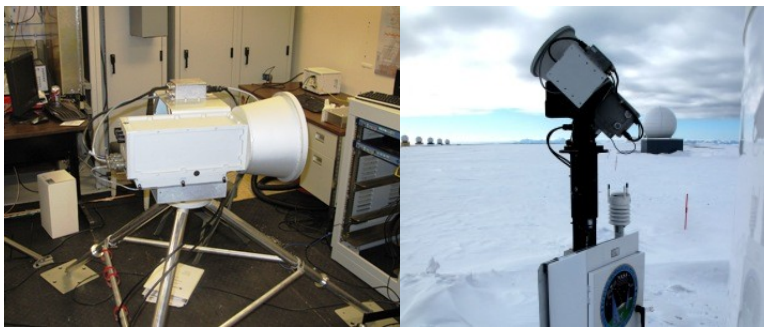

Fig. 1. Photographs of the radiometer system during system-check and after deployment at the operational site in Longyearbyen, Norway

Table 1. Characteristics of the Microwave Radiometer

Parameter	Specification
Operating Frequencies	25.5 – 26.5 GHz
RF bandwidth	>1 GHz
IF bandwidth	500 MHz
Half power beam width of horn antenna	3 degrees
Sidelobes	< - 25dB
Integration Time	10 – 2500 msec
Input Range	0 – 313 K
Sensitivity	0.5 K
Accuracy	0.1 - 1 K
Long Term Stability	< 1 K per 180 days
Noise figure	Mixer-preamplifier 4.0 dB Isolator 0.3 dB Filter 0.2 dB Latching circulator 0.3 dB Waveguide 0.2 dB Total 5.0 dB
Receiver Type	Super heterodyne
Switch	Dicke Type
Weight	20 Lbs
Op. Temp. Air Temp.	-50 - +50 Deg. C.
Power Supply	120V, 60 Hz at 5 Amps

The radiometer measures the antenna noise temperature T_{ant} , which differs from the sky brightness temperature T_b because the antenna 'sees' both the sky at temperature T_b and the ground at temperature T_g. Thus, T_{ant} is a linear combination of the sky and ground temperatures:

(2)

where H is the fraction of power received by the main beam. H can be estimated with good accuracy from the antenna pattern. If H and T_g are known, T_b is calculated by inverting equation (2):

(3)

The path attenuation is estimated from the radiometric brightness temperature (T_b) through the following equation:

(4)

where T_{med} is the effective medium sky temperature in Kelvin and T_c is the cosmic background temperature also in Kelvin, usually taken to be around 2.75. The value for T_{med} is usually estimated by using a model of the atmosphere along with surface meteorological measurements (e.g., surface temperature, relative humidity and barometric pressure) **[5].** In this paper we are assuming T_{med} to be 275 Kelvin.

Figure 2 shows the tipping curve obtained shortly after deployment of the microwave radiometer in Longyearbyen, Norway. The correlation coefficient was greater than 99.8%, which is considered to be very good for a scanning radiometer operating at Ka-Band. The radiometer calculates the tipping curve at least twice a day and will adjust the system parameters if the correlation coefficient goes below 97%.

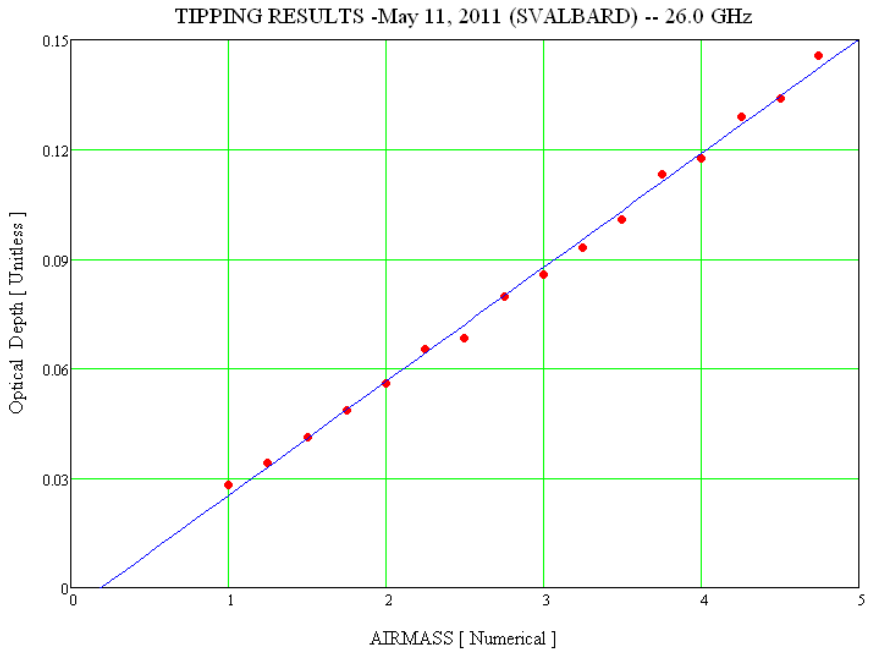

Fig. 2. Example of a tipping calibration curve depicting the linear relationship between airmass (elevation angle dependant) and optical depth achieved by the radiometer system.

I. Statistical Results

Presented in **Figure 3** are the overall cumulative distribution functions (CDF) of the measured sky brightness temperature (with reference to zenith) at 25.5, 26.0, 26.3 and 26.5 GHz, and the corresponding attenuation CDFs from one month of data collection (May 2011).

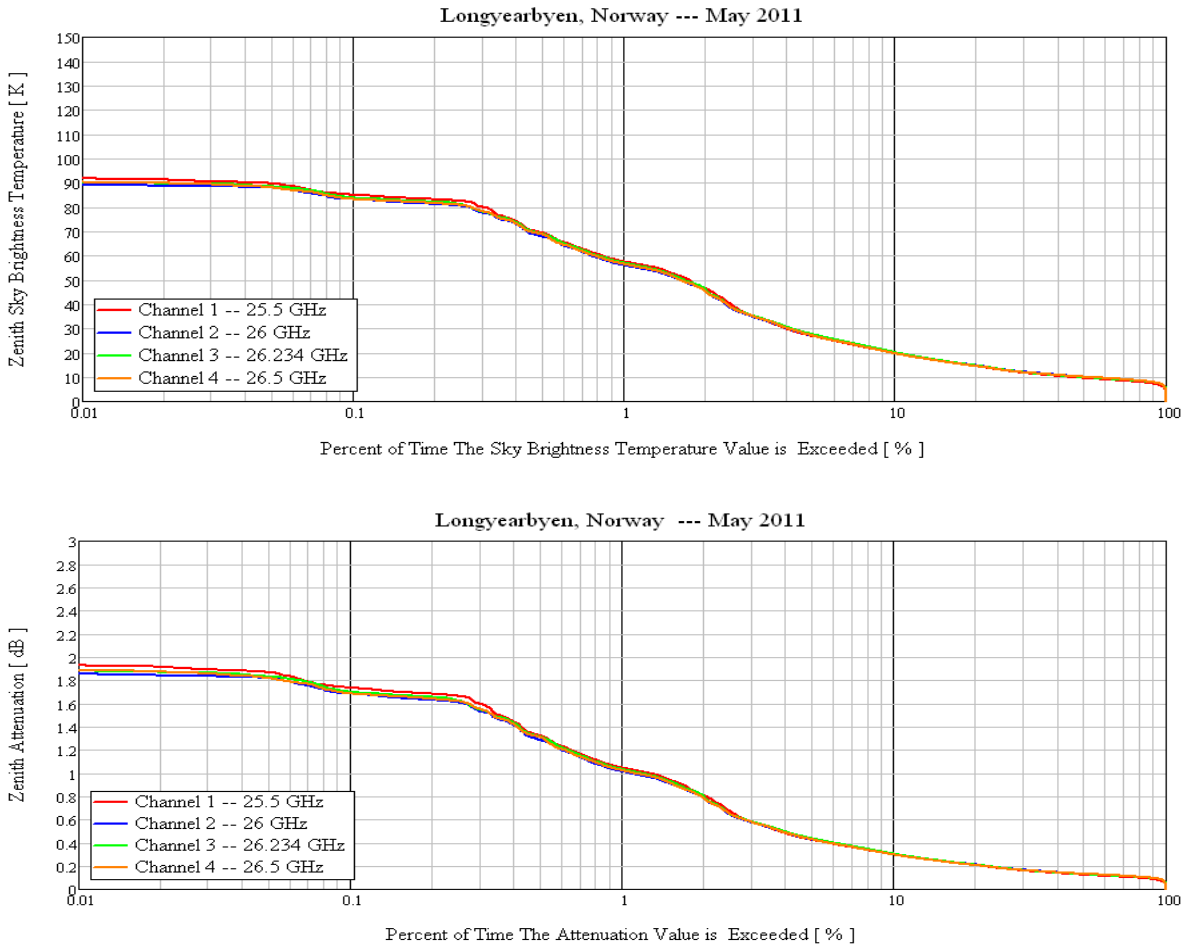

Fig. 3. *Upper,* Cumulative distribution functions of the zenith sky brightness temperature. *Lower,* Cumulative distribution functions of the zenith attenuation.

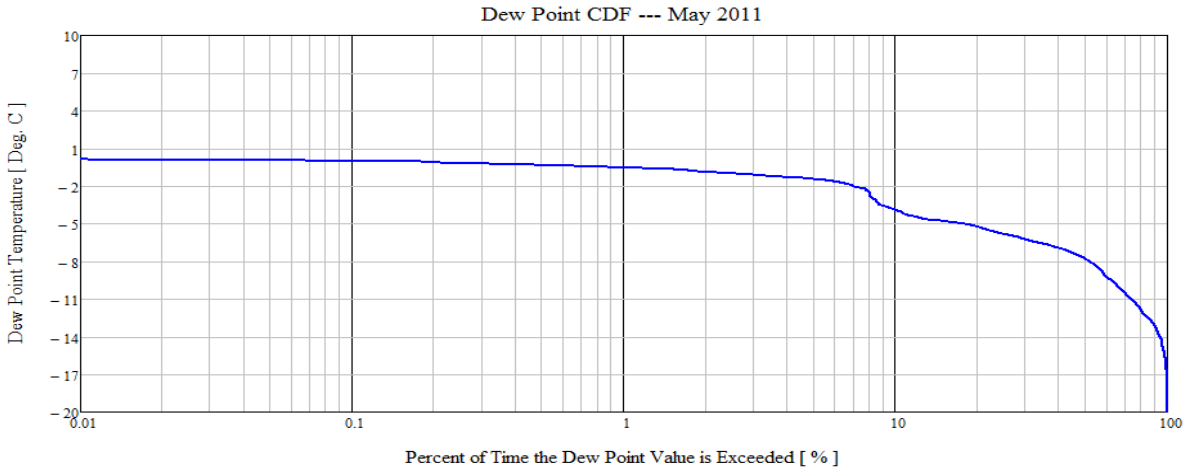

Fig. 4. Cumulative distribution function of the dew point temperatures for May 2011 at Longyearbyen, Norway.

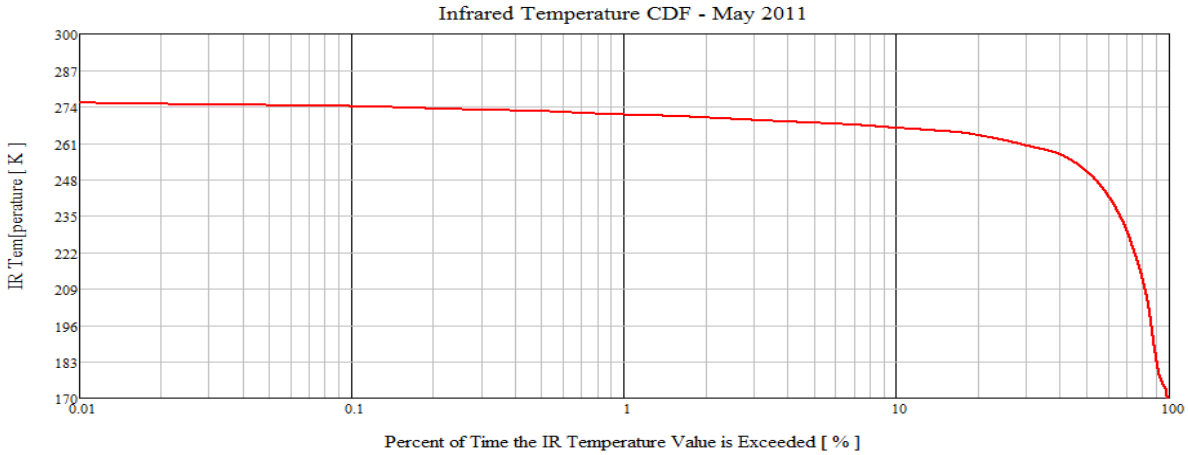

Fig. 5. Cumulative distribution of the IR temperature at zenith for May 2011 at Longyearbyen, Norway.

From **Figure 3**, we observed that the 90th percentile for the zenith attenuation is about 0.3 dB, the 99th percentile 1.0 dB and 99.9th percentile is 1.7 dB. The low measured attenuation statistics can be explained by noticing that during the month of May, Longyearbyen experienced very low dew point temperatures (see **Figure 4**). It is well known that a low dew point in the absence of precipitation implies very low content of perceptible water vapor (PWV) **[6]** and therefore very low attenuation from gaseous absorption and clouds. **Figure 5** shows that there was strong cloud cover for a majority of the time in May 2011, but the measured contribution in attenuation due these clouds was very minimal, most likely due to lack large water content in them.

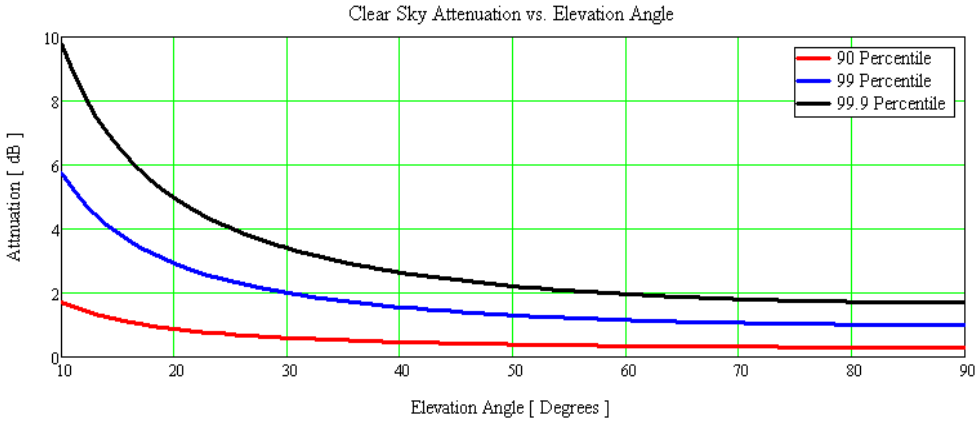

Fig. 6. Clear sky attenuation versus elevation angle at 90, 99 and 99.9 Percentile.

Assuming that the stratified layers in the atmosphere are homogeneous the attenuation statistics can be extrapolated to various elevations angles Figure 6 shows the variability of the attenuation statistics as a function elevation angle at three different percentiles (90, 99 and 99.9, respectively).

II. Conclusive Remarks and Future Work

From one month of data collection in Longyearbyen, Norway, the statistics show minimal measured signal attenuation by gaseous absorption (oxygen and water vapor) and clouds. This is most likely due the low content of precipitable water vapor in the atmosphere during the month of May. No rain was recorded during the measurement period, but precipitation will increase attenuation where it occurs in future measurements. A statistically meaningful analysis for this site is not possible with only one month of data collection, but preliminary results indicate that the site is very well suited for Ka-band operations. A more comprehensive characterization will be done after several years of data collection have been conducted.

III. VI. References

[1] E. K. Smith., “Centimeter and Millimeter Wave Attenuation and Brightness Temperature due to Atmospheric Oxygen and Water Vapor,” Radio Science, Vol. 17, Number 6, pages 1455-1464, Nov. – Dec., 1982.

[2] M. E. Tiuri, “Radio Astronomy Receivers,” IEEE Transactions on Military Electronics, July-October, 1964.

[3] V. R. Reddy, “13.9 GHz Radiometer Design,” The University of Kansas Center for Research, Inc, RSL TR 3311-3, October 1984.

[4] Y. Han and E. R. Westwater, “Analysis and Improvement of Tipping Calibration for Ground-Based Microwave Radiometers,” IEEE Transactions on Geoscience and Remote Sensing, Vol.38, No. 3, May 2000.

[5] H. J. Liebe, “Modeling Attenuation and Phase of Radio Waves in Air at Frequencies below 1000 GHz,” Radio Science, 16(6), pages 1183-1199, 1981.

[6] F.T. Ulaby, R.K. Moore and A.K. Fug, Microwave Remote Sensing: Active and Passive, Vol. 1 and Vol. 2, Microwave Remote Sensing Fundamentals and Radiometer, Addison-Wesley, Reading, Mass., 1981.